24th INTERNATIONAL CONGRESS ON SOUND AND VIBRATION
23–27 July 2017, London

ICSV24
23-27JULY 2017
LONDON CALLING

EXPERIMENTALLY BASED STATISTICAL ANALYSIS OF THE VIBRATIONAL ENERGY OF CLT BUILDING ELEMENTS

Simon Mecking, Markus Scheibengraber, Tobias Kruse, Ulrich Schanda and Ulrich Wellisch

Laboratory for Sound Measurement LaSM, University of Applied Sciences Rosenheim, Hochschulstr. 1, 83024 Rosenheim, Germany.

email: simon.mecking@fh-rosenheim.de

The prediction of sound insulation of buildings is standardised in EN 12354. The method is based on a simplified Statistical Energy Analysis (SEA) approach. The energy ratios of various subsystems are the main quantities to predict sound transmission. The method has proven to work sufficiently accurate for masonry and concrete buildings, where the building components like walls, floors etc. can be regarded as rather homogeneous structures. To adapt this method for solid timber constructions it is necessary to prove that basic SEA requirements are fullfilled by orthotropic materials and heterogeneous structures that occur in these building types. In a case study, an isolated T-junction formed by Cross Laminated Timber (CLT) elements is experimentally investigated. The buildings elements are subdivided in segments with typical screwed connections. In the experiments the diffusivity of the vibration field is investigated, using point excitation with a shaker at several positions and many, randomly chosen response positions. MONTE-CARLO simulations are conducted for random but fix-sized subsets of the measured response positions to find the necessary number of response positions for an accurate determination of the vibrational energy. As a result the distribution of the mean velocity levels can be approximated. In a second approach a multiple linear regression model based on the least absolute shrinkage and selection operator (LASSO) is applied, because for lower frequency bands multicollinearity is expected. In the context of linear regression modelling, data-driven methods are used to select optimal subsets of response positions, to get an estimating equation.

Keywords: Statistical Energy Analysis, Cross Laminated Timber, LASSO, Regression model, Bootstrap prediction interval

1. Introduction

For the prediction of sound insulation in buildings, knowledge about the relevant energy transfer paths is essential. These depend on the physical properties of the involved components and their coupling. Some assumptions in EN 12354:2000 are based on junction properties and the bending stiffness of the plates which are typical for masonry and concrete constructions. Additionally the measurement procedure described in ISO 10848-1:2006 [1] is harmonised to these constructions. This standard gives guidance for the number and the positions of responses and of excitation positions to quantify the vibrational energy E_{vib} of a component, for example. E_{vib} is experimentally determined by a temporal and spatial average of the squared velocity $\langle v_{\text{eff}} \rangle^2$ and the total mass m according to (1). Thereby I is the total number of the individual response positions i, E_{kin} the kinetic energy and E_{pot} the potential energy of the component.

$$E_{\text{vib}} = 2\,E_{\text{kin}} = m\,\langle v_{\text{eff}} \rangle^2 = \frac{1}{I}\sum_{i=1}^{I} m_i\,v_{\text{eff},i}^2 \tag{1}$$

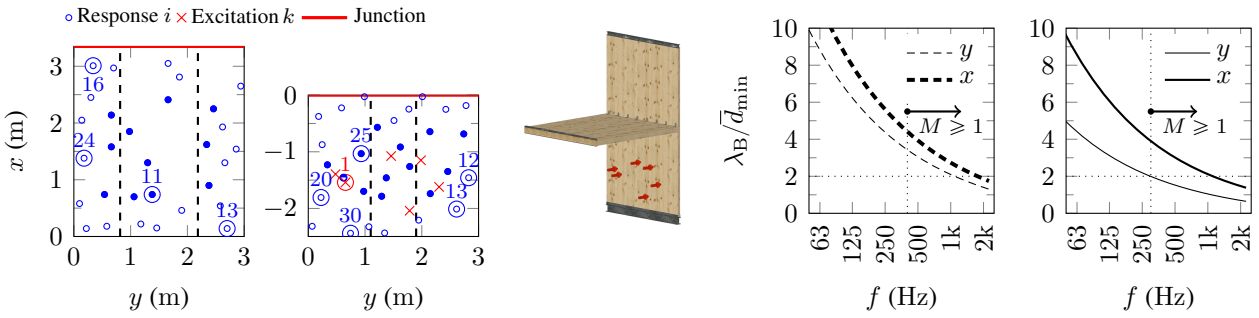

(a) Top view of floor (left) and side view of wall (right). The dashed lines on the buildings components indicate the positions of the connections of the single CLT elements. The numbered response positions are the optimal subsets acc. to (11) and (12).

(b) Test rig

(c) Spatial sampling of floor (left, $\overline{d}_{\text{min}} = 0.400\,\text{m}$) and wall (right, $\overline{d}_{\text{min}} = 0.401\,\text{m}$). The bending wavelength λ_B for both principal directions is normalised to the averaged, minimum distance $\overline{d}_{\text{min}}$ between two adjacent response positions. The modal overlap factor $M \geqslant 1$ is also drawn.

Figure 1: Test rig consists of CLT elements. Six different excitation positions and 30 response positions ○● (model B: only ●) are used on the floor and bottom wall, respectively. The floor intersects the two walls.

There are different assumptions for (1). The two conditions listed below will be focused:

1. $E_{\text{kin}} = E_{\text{pot}}$
2. Number of response positions I
   (a) Non-diffuse vibration field: $I \to \infty$
   (b) Nearly diffuse field: Minimum number of uniformly distributed positions $I \to I_{\text{min}}$

The first assumption is justifiable at the resonance frequency of a mode or approximately within a frequency band that contains many modes. The second assumption is experimentally impractical; except for the case of a nearly diffuse vibration field the number of required response positions is sensible due to its low spatial variation.

From a physical point of view solid wood constructions show some fundamental differences to classical heavyweight constructions. In the case of Cross Laminated Timber (CLT) the material stiffness can have a strong directional dependency. Additionally the junctions between building components can be regarded as point connected and are more flexible. To adapt SEA-based models for solid wood constructions it is therefore necessary to verify calculated energy quantities by experiments.

The questions are (a) whether an adaption of the measurement procedure for these components is necessary to estimate the vibrational energy for a chosen confidence interval and (b) how to consider physical characteristics of those components. To find an answer to these questions an experiment [2] and a statistical evaluation of the vibration field [3] are performed. For statistical analysis the software R is used [4] with the packages BOOT [5] and LARS [6].

2. Case study on a T-shaped junction of components

2.1 Test rig and measurement setup

The vibroacoustic test rig at the University of Applied Sciences Rosenheim has been developed to determine vibration reduction indices of solid timber building elements by Operational Vibration Analyses and the Power Injection Method. It is possible to investigate T- and L-shaped junctions of typical building dimensions with the possibility of applying an extra load per unit length of $20\,\text{kN/m}$ maximum. Figure 1 (b) shows the T-shaped junction regarded within this case study consisting of two CLT walls and one floor. The walls have three and the floor six crosswise glued layers.

To excite the structure a modal shaker was used driven with a logarithmic sinus-sweep signal ($2\,\text{oct}\,/\,\text{min}$). In the experiments the force and acceleration at the excitation positions as well as the acceleration of the response positions shown in Fig. 1 (a) are measured. For the statistical analysis the

bottom wall is excited and the energy of the floor is determined. For the excitation positions the area nearby the edges according to [1] and the centre lines are excluded before using a random choice at the bottom wall. For each of the six excitation positions the identical sample of 30 response positions is used. The response positions are chosen stepwise by chance, but keeping a minimum distance around already fixed positions.

Figure 1 (c) gives information about the average spatial sampling in x- and y-direction using the chosen response positions. For long bending waves high spatial level differences cannot be avoided because of the modal vibration pattern at low frequencies. However in the mid frequency range the spatial level differences are declining, since the vibration field becomes more diffuse due to the fact that the number of modes per band and the inter-modal energy exchange are increasing. For the evaluation of energy equipartition the modal overlap factor $M \geqslant 1$ is added to Fig. 1 (c). In compliance with the theorem of SHANNON the ratio between the bending wavelength λ_B and the average distance of response position $\overline{d}_\mathrm{min}$ has to be bigger than 2, but it is expected that this condition becomes less important with increasing modal overlap factor.

2.2 Results of experiment

The characteristics of the excitation positions k are illustrated by the driving-point mobility $L_{Y,k}$ for an one-third octave band f. It is calculated from narrow-band measurements with J frequency steps according (2), where the reference mobility Y_0 is $1\,(\mathrm{m/s})/\mathrm{N}$. Figure 2 (a) shows a significant effect of the excitation position below $250\,\mathrm{Hz}$. Especially the results in the one-third octave bands $50\,\mathrm{Hz}$ and $80\,\mathrm{Hz}$ show a wide scattering, probably due to a spatial selective excitation of modes.

$$L_{Y,k} = 20\lg\left(\frac{1}{Y_0}\frac{1}{J}\sum_{j=1}^{J}\mathrm{Re}\left\{\frac{\underline{v_{k,j}}}{\underline{F_{k,j}}}\right\}\right) \tag{2}$$

An analysis of the driving-point mobilities in narrow bands has shown that no modes were excited in the one-third octave bands $63\,\mathrm{Hz}$ and $125\,\mathrm{Hz}$. In these frequency bands the prerequisite $E_\mathrm{kin} = E_\mathrm{pot}$ for the application of (1) is not fulfilled. To minimise the effect of different force amplitudes at the excitation positions k, the narrow-band velocity $\underline{v_{i,k,j}}$ at response position i is normalised to the force $\underline{F_{k,j}}$ and summed in an one-third octave band $\overline{f}$ according to (3). With the reference velocity $v_0 = 1 \times 10^{-9}\,\mathrm{m/s}$ the spatial average velocity level $L_{\langle v\rangle,\mathrm{norm},k}$ is calculated according to (4).

$$v^2_{\mathrm{norm},i,k} = \sum_{j=1}^{J}\left|\frac{\underline{v_{i,k,j}}}{\underline{F_{k,j}}}\right|^2 1\,\mathrm{N}^2 \tag{3}$$

$$L_{\langle v\rangle,\mathrm{norm},k} = 10\lg\left(\frac{1}{v_0^2}\frac{1}{I}\sum_{i=1}^{I} v^2_{\mathrm{norm},i,k}\right) \tag{4}$$

Figure 2 (b) shows these results for the wall and the floor respectively. The discrepancies between results of different excitation positions again are significant below $250\,\mathrm{Hz}$ due to the spread of the driving-point mobilities. Above $250\,\mathrm{Hz}$ the effect of the excitation position on the spatial average velocity level is insignificant for the CLT-wall and floor.

The box plots in Figs. 2 (c) and (d) illustrate the distribution and the spread of the 30 individual normalised velocity levels for the specific excitation position $k = 1$. Especially at low and high frequency bands a wide variance and an asymmetrical distribution can be observed. At low frequencies this indicates a non-diffuse vibration field resulting from the modal behaviour of the components. At high frequencies three effects lead to the non-diffuse vibration field: the increasing influence of the direct field around the excitation position, the decrease in vibrational energy with distance and the weak coupling between the single elements of the components. In the mid-frequency range from $200\,\mathrm{Hz}$ to $1250\,\mathrm{Hz}$ the interquartile range of the box plots are significantly smaller, which indicates a

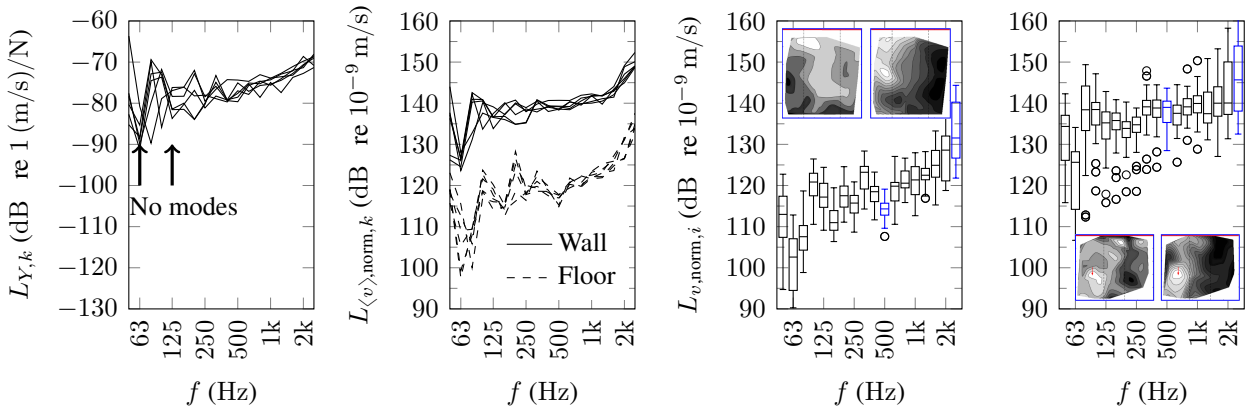

(a) Driving-point mobilities of the wall

(b) Spatial average velocity levels ($I = 30$)

(c) Box plots of all velocity levels at floor

(d) Box plots of all velocity levels at wall

Figure 2: Results of measurement in one-third octave bands for each excitation position k in (a),(b) and for $k = 1$ in (c),(d). The examples (left: $f = 500\,\mathrm{Hz}$, right: $f = 2.5\,\mathrm{kHz}$) of spatial level differences in (c),(d) are related to the minimal level $\min\left(L_{v,\mathrm{norm},i}\right)$ of the component. [2]

nearly diffuse vibration field. In case of the point excited wall in Fig. 2 (d) there are more statistical outliers. Two of the thirty measured response positions are located in the vicinity of the junction between wall and floor. These positions led to some of the statistical outliers with low values.

3. Statistical analysis of the vibration fields

3.1 Monte-Carlo simulation

Let $I \in \mathbb{N}$ be the total number of measured response positions on the component and $N \in \mathbb{N}$ the size of an arbitrary subset. Furthermore let $R \in \mathbb{N}$ denote the total number of repetitions of the drawing procedure and let $v_{\mathrm{norm},i}$ with $i = 1, 2, \ldots, I$ denote the measured velocity on the i-th response position in a frequency band f. The complete statistical analysis in this section is based on the assumption that $R = 200\,000$ is sufficiently large to apply the law of large numbers [7, p. 343] and the theorem of Glivenko-Cantelli [8, p. 98]. Different situations are modelled:

3.1.1 Model A: Drawing from all response positions

Firstly the distribution of the spatial average velocity level has to be examined by drawing a fixed-sized subset with size N from all measured response positions for a particular frequency band f. Thereby a random variable $L^{(N)}_{\langle v\rangle *}$ is constructed to predict the spatial average velocity level for the respective component if only $N \leqslant I$ response positions are used for an excitation position k. In (5) the set $\Omega^{(N)}$ describes all possible random combinations of velocity levels for the drawing without replacement.

$$
\begin{aligned}
&L^{(N)}_{\langle v\rangle *} : \Omega^{(N)} \to \mathbb{R}, \quad L^{(N)}_{\langle v\rangle *}(\omega) = 10\lg\left(\frac{1}{v_0^2}\frac{1}{N}\sum_{n=1}^{N}\omega_n^2\right) \\
&\text{with } \Omega^{(N)} = \bigotimes_{n=1}^{N}\Omega_n \setminus \left\{\omega \in \bigotimes_{n=1}^{N}\Omega_n : \exists l, m \in \{1,\ldots,N\} : l \neq m \wedge \omega_l = \omega_m\right\} \\
&\text{and } \Omega_n = \{v_{\mathrm{norm},1}, v_{\mathrm{norm},2}, \ldots, v_{\mathrm{norm},I}\} \text{ for } n = 1, 2, \ldots N.
\end{aligned}
\tag{5}
$$

Based on this model the distribution of the spatial average velocity levels can be approximated. From this approximation the minimum number of randomly chosen response positions $N_{\min,k}$ can be

(a) Floor (b) Wall

Figure 3: Minimum number $N_{\min,k}$ of responses that $L_{\langle v\rangle,\text{norm},k} \pm 2\,\text{dB}$ is the 95%-prediction interval for $L^{(N)}_{\langle v\rangle*,k}$ depending on the different excitation position k as result of the MONTE-CARLO simulation (model A).

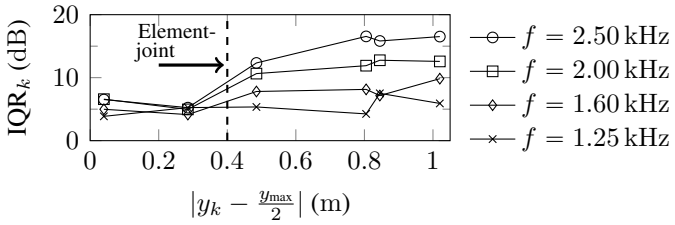

Figure 4: Impact of the y-distance between excitation position k and the centre line of the component $\frac{y_{\max}}{2}$ on the interquartile range IQR_k of the velocity levels $L_{v,\text{norm},i,k}$.

derived for the different excitation positions k to have an acceptable deviation from the spatial average velocity level of all response positions, see Fig. 2 (b).

Figure 3 shows the minimum numbers of response positions to guarantee a maximum deviation of $2\,\text{dB}$ with a probability of at least $p \geqslant 0.95$. In addition to $N_{\min,k}$ of the used excitation positions also the average value over the excitation positions is drawn as a trend line. The minimum numbers $N_{\min,k}$ of the floor and wall show a similar frequency dependency. In the non-diffuse frequency range more response positions are necessary compared to the frequency range with a nearly diffuse vibration field. The differentiation of the diffusivity is based on the interquartile ranges of the box plots in Figs. 2 (c) and (d). A strong impact of the excitation position on $N_{\min}$ can be observed at high frequencies. This is caused by the different distance of position k to the centre of the component in y-direction. Figure 4 shows the interquartile range IQR_k of the velocity levels depending on this distance. Above $1.25\,\text{kHz}$ the width of the interquartile range is increasing with the frequency if the excitation position is on the left or on the right element of the wall built from three segments.

3.1.2 Model B: Drawing from response positions excluding the boundary/near-field area

For practical applications it is useful to know, how many response positions are necessary to guarantee a deviation $t_{\max}$ for several frequency bands. In this example $f_{\min} = 200\,\text{Hz}$ is the lowest and $f_{\max} = 1250\,\text{Hz}$ the highest one-third octave band of the interesting frequency range. In this drawing procedure response positions in the vicinity of the component edges and close to the excitation position are not considered. Only the response positions with the filled circle in Fig. 1 (a) are used for sub-sampling in this model. I^* represents the total number of these response positions. The minimum distances for valid response positions in Table 1 are based on the bending wavelength λ_B at $f_{\min}$ and the radius of the nearfield at $f_{\max}$ of the particular components [9].

The following model is an estimation for the probability that the average velocity level determined from an arbitrary, fixed sized subset of $N = 6$ response positions deviates at most $t_{\max} \in \mathbb{R}^+$ from the average velocity level calculated by all measured response positions I (denoted by $L_{\langle v\rangle,\text{norm},f}$) for the frequency band f. The deviation is applied to the average velocity level of all response positions for

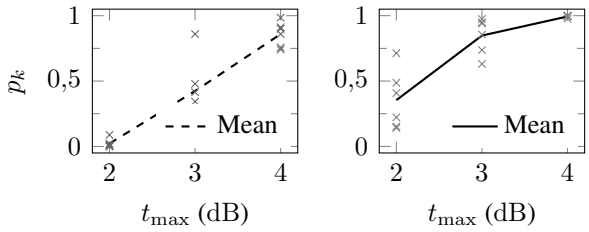

(a) Floor (b) Wall

Figure 6: Probability p_k for model B that the mean velocity level determined from any arbitrary subset of $N = 6$ response positions differs less than $t_{\max}$ to the level of all response positions $I = 30$.

Table 1: Minimum distances of response positions to edges of the building components and to excitation position for model B.

	$x_{\min}$	$y_{\min}$	$r_{\min}$
		m	
Wall	0.51	0.26	0.19
Floor	0.67	0.52	–
Criterion	$\frac{\lambda_{\mathrm{B},x}}{4}$ (200 Hz)	$\frac{\lambda_{\mathrm{B},y}}{4}$ (200 Hz)	r_{H} (1.25 kHz)

every one-third octave band in the frequency range from $f_{\min}$ to $f_{\max}$. $B^{(N)}$ is a dichotomous random variable with value 1 if $\omega \in Z$ and value 0 if $\omega \notin Z$.

$$B^{(N)} : \Omega^{(N)} \to \{0,1\}, \quad B^{(N)}(\omega) = \prod_{f=f_{\min}}^{f_{\max}} \mathbb{1}_Z(\omega)$$

$$\text{with } \Omega^{(N)} = \{1,\ldots,I^*\}^N \backslash \{\omega \in \{1,\ldots,I^*\}^N : \exists l,m \in \{1,\ldots,N\} : l \neq m \wedge \omega_l = \omega_m\}, \quad (6)$$

$$Z := \left\{ \omega \in \Omega^{(N)} : \left| 10\lg\left(\frac{1}{v_0^2}\frac{1}{N}\sum_{n=1}^{N} v^2_{\mathrm{norm},f,\omega_n}\right) - L_{\langle v\rangle,\mathrm{norm},f} \right| \leqslant t_{\max} \right\}.$$

Figure 6 shows the probabilities as results of the distributions depending on the permissible deviation. The deviation have to be fulfilled in all of the nine frequency bands. In case of the floor the probabilities become high only for a high chosen deviation $t_{\max} \leqslant 4\,\mathrm{dB}$, but in case of the bottom wall already for a smaller deviation of $t_{\max} \leqslant 3\,\mathrm{dB}$. The more inconvenient spatial distribution of the response positions of the floor in Fig. 1 (a) could potentially be an explanation for the lower probabilities.

3.2 Linear regression model

The MONTE-CARLO simulations are not suitable to give a proposal for a data-driven optimal subset relating to the prediction of the spatial average velocity level of the component. To find automatically such an optimal subset with statistical techniques a linear regression model is built up. Instead of the well-known mean squared estimation [10, p. 44-49] of the regression coefficients, the least absolute shrinkage and selection operator (LASSO) [10, p. 68-69] is used here to estimate the coefficients in the linear regression model. LASSO is a penalised form of the mean squared estimation. The LASSO estimation for regression coefficients is selected, because there is a smaller variance in the case of nearly multicollinear input vectors [10, p. 61], what could be present due to the spatial correlations in our experimental setting.

3.2.1 LASSO estimation of regression coefficients

The LASSO estimator for the regression coefficients $\beta = (\beta_1,\ldots,\beta_I)^T$ is defined in [10, p. 68]:

$$\hat{\beta}^{LASSO} = \underset{\beta}{\operatorname{argmin}} \left\{ \sum_{s=1}^{S}(y_s - \sum_{i=1}^{I} x_{si}\beta_i)^2 + \lambda \sum_{i=1}^{I} |\beta_i| \right\} \text{ with } \lambda \geqslant 0. \quad (7)$$

s stands for the number of observation ($S = 2$). For $\lambda = 0$ the LASSO estimation is equal to the ordinary mean-squared estimation. For simplicity a multiple linear regression with LASSO estimation is called in the following LASSO regression.

To apply LASSO regression to this case study the output vector y in (8) consists of the spatial average velocity levels $L_{\langle v\rangle,\text{norm},s,f}$ for the respective frequency band f and measurement repetition s. The input vectors x_i in (9) consist of the velocity levels $L_{v,\text{norm},i,s,f}$ of the i-th response position.

$$y = (L_{\langle v\rangle,\text{norm},1,f_{\min}}, \ldots, L_{\langle v\rangle,\text{norm},1,f_{\max}}, L_{\langle v\rangle,\text{norm},2,f_{\min}}, \ldots, L_{\langle v\rangle,\text{norm},2,f_{\max}})^T \tag{8}$$

$$x_i = (L_{v,\text{norm},i,1,f_{\min}}, \ldots, L_{v,\text{norm},i,1,f_{\max}}, L_{v,\text{norm},i,2,f_{\min}}, \ldots, L_{v,\text{norm},i,2,f_{\max}})^T \tag{9}$$

The structural form of the LASSO regression model is defined in (10).

$$y = \beta_1 x_1 + \beta_2 x_2 + \ldots + \beta_I x_I + e. \tag{10}$$

e is a random error vector with expectation 0 and homogeneous variance greater 0 for the vector components. (10) means that the normalised spatial average velocity level can be written as a linear combination of the normalised velocity levels in all response positions. Before the determination of the regression coefficients β_i with LASSO it must be proved if a reduction of response positions in the LASSO regression is feasible. This is done in the next step.

3.2.2 Model size reduction to find an optimal submodel

In [3, p. 76-82] the author describes four different methods to gradual include response positions into the LASSO regression model. In this case study only the variable selection with respect to the Akaike Information Criteria (AIC) is applied.

The model selection starts with a single response position in the model. Further response positions are added as long as the prediction interval is greater than $2\,\text{dB}$ in at least one frequency band. The model selection is executed for the excitation position $k = 1$. In case of the floor the resulting sequence of response positions is [24,11,16,13] for $f = 100\,\text{Hz}$ to $1250\,\text{Hz}$ with a maximum 95%-prediction interval width of $1.96\,\text{dB}$ and in case of the wall the sequence for $f = 80\,\text{Hz}$ to $1250\,\text{Hz}$ is [25,30,12,13,20] with a maximum 95%-prediction interval width of $1.67\,\text{dB}$. Because in both cases only very small subsets (Fig. 1 (a)) of all measured response positions are selected, the LASSO regression models have not the situation of nearly multicollinear input vectors. Therefore the LASSO estimation is performed as ordinary mean squared estimation for the regression coefficients. In this case the algorithm in [11, p. 285] can be used to calculate the prediction intervals.

With the chosen models the regression coefficients and bootstrap confidence intervals for the coefficients (see [3, p. 83]) are calculated. The total number of bootstrap replications is chosen as $R_{\text{Bootstrap}} = 8000$. In case of the floor the estimating equation for each one-third octave band f between $f_{\min}$ and $f_{\max}$ is (11) and in case of the wall (12).

$$\begin{aligned}\mathbb{E}(L_{\langle v\rangle,\text{norm},s,f}) =& 0.232(\pm 0.080)\, L_{v,\text{norm},i=24,s,f,k=1} + 0.401(\pm 0.049)\, L_{v,\text{norm},i=11,s,f,k=1} \\ &+ 0.251(\pm 0.067)\, L_{v,\text{norm},i=16,s,f,k=1} + 0.123(\pm 0.045)\, L_{v,\text{norm},i=13,s,f,k=1}\end{aligned} \tag{11}$$

$$\begin{aligned}\mathbb{E}(L_{\langle v\rangle,\text{norm},s,f}) =& 0.126(\pm 0.083)\, L_{v,\text{norm},i=25,s,f,k=1} + 0.173(\pm 0.026)\, L_{v,\text{norm},i=30,s,f,k=1} \\ &+ 0.431(\pm 0.065)\, L_{v,\text{norm},i=12,s,f,k=1} + 0.158(\pm 0.050)\, L_{v,\text{norm},i=13,s,f,k=1} \\ &+ 0.127(\pm 0.048)\, L_{v,\text{norm},i=20,s,f,k=1}\end{aligned} \tag{12}$$

4. Conclusion

The diffusivity of the vibration fields of CLT-components and the frequency distributions depending on the number of responses are described by empirical data and MONTE-CARLO methods. In this case study a nearly diffuse vibration field is available only in some one-third octave bands at mid frequency range. It follows that the determination of energy with few response positions is only possible

in this frequency range. The determination of energy by velocity is not suitable in frequency bands without modes. Because in this case the prerequisite of consistency between kinetic and potential energy is not fulfilled. At high frequencies the position of excitation relating to the position of the joints of elements in plane has a significant impact on the scattering of the responses. Above all a high number of responses is necessary at low and high frequencies.

In a second approach an optimal subset of response positions to estimate the average velocity level could automatically be determined using a linear regression model with LASSO estimation. The corresponding regression coefficients are calculated with bootstrap confidence intervals. The LASSO regression also enables to calculate bootstrap prediction intervals. The regression results can be used for repetition measurements, where only the optimal subset of measurement positions is used. Thus it spares the measurement of all response positions in the repetition measurement, because it can be guaranteed that the spatial average velocity level for all positions is within the prediction interval with a corresponding confidence level.

Acknowledgment

The results are based on the current status of the research project *Vibroacoustics in the planning process for timber constructions* (No. 18724N) funded by the German Research Foundation (DFG) and German Federation of Industrial Research Associations (AIF). It is carried out by Technical University Munich, ift Rosenheim and University of Applied Sciences Rosenheim.

REFERENCES

1. ISO 10848-1:2006-08. *Acoustics - Laboratory measurement of the flanking transmission of airborne and impact sound between adjoining rooms*.

2. Kruse, T., *Messung und Analyse des Schwingungsverhaltens von gekoppelten Bauteilen aus Brettsperrholz*, Master's thesis, University of Applied Sciences Rosenheim, (2016).

3. Scheibengraber, M., *Simulative Untersuchung der Variabilität des Körperschallfeldes im Holzmassivbau unter Anwendung der Ridge Regression und dem Least Absolute Shrinkage Operator (Lasso) als restringierte Formen des linearen Modells*, Bachelor's thesis, University of Applied Sciences Rosenheim, (2016).

4. R Core Team, *R: A Language and Environment for Statistical Computing*, Vienna, Austria (2016).

5. Canty, A. and Ripley, B., *boot: Bootstrap R (S-Plus) Functions*, R package v.1.3-18 (2016).

6. Hastie, T. and Efron, B., *lars: Least Angle Regression, Lasso and Forward Stagewise*, R package v.1.2 (2013).

7. Pruscha, H., *Vorlesungen über Mathematische Statistik*, Teubner, Stuttgart, Germany (2000).

8. Lehn, J. and Wegmann, H., *Einführung in die Statistik*, Teubner, 5. Aufl., Wiesbaden, Germany (2006).

9. Mecking, S., Kruse, T., Châteauvieux-Hellwig, C. and Schanda, U. Körperschallfelder in Brettsperrholzbauteilen des Holzmassivbaus, *Proceedings of Fortschritte der Akustik - DAGA 2016*, Deutsche Gesellschaft für Akustik e.V.

10. Hastie, T., Tibshirani, R. and Friedman, J., *The elements of statistical learning*, Springer, New York, USA (2009).

11. Davison, A. C. and Hinkley, D. V., *Bootstrap methods and their application*, Cambridge University Press, 11th printing., Cambridge, UK (2009).